

# Raman Measurements and Stress Analysis in Gallium Ion Implanted Gallium Nitride Epitaxial Layers on Sapphire

S. Mal<sup>a</sup>, A. Singha<sup>a</sup>, S. Dhara<sup>b</sup>, A. Roy<sup>a\*</sup>

<sup>a</sup>*Department of Physics, Indian Institute of Technology Kharagpur 721302, West Bengal, India*

<sup>b</sup>*Institute of Atomic and Molecular Sciences, Academia Sinica, Taipei 106, Taiwan*

## Abstract

In this article, we estimate hydrostatic stress developed in gallium ion implanted gallium nitride epitaxial layers using Raman measurements. We have calculated deformation potential constants for  $E_2(\text{high})$  mode in these epi-layers. The presence of a polar phonon-plasmon coupling in these systems has also been demonstrated. In as-implanted samples, with an increase in implantation fluence, we have observed disorder-activated Raman scattering.

## 1. Introduction

Wurtzite structure Gallium Nitride ( $h$ -GaN) epitaxial layers (epi-layers) are direct wide band gap ( $\sim 3.4$  eV) two dimensional semiconductor systems which have applications in optoelectronic and microelectronic devices operating in the blue and ultraviolet. In GaN-based devices, ion-implantation is an attractive technique for selective-area doping, precise control over dopant concentration etc. Above a threshold fluence, ion-implantation leads to formation of cubic ( $c$ -GaN, space group  $T_d^2$ ) phase, which has many advantages over  $h$ -GaN (space group  $C_{6v}^4$ ) [1]. The ion irradiation knocks out atoms from the irradiated material and creates point defects in the lattice. It does not create any massive damage and large defect complexes. It is to be noted that the important point defects, caused by ion-irradiation, are vacancies and interstitials. These defects induce localized electron energy levels into the band gap of the host semiconductor and hence results in a change in the electrical properties of the material. In addition, these defect states interact with light, inducing an increase in absorption or emission of photons in radiative recombination processes [2, 3, 4, 5]. It has been claimed that the atomic structure of the defect states are respon-

sible for the yellow emission in GaN [6]. Strain in the lattice (due to lattice mismatch, difference in thermal coefficient, incorporated impurities, and point defects) is an important issue in fabricating optoelectronic devices.

Stress-strain relation in virgin *h*-GaN layer is well-studied in the literature [7]. In this article, we discuss Raman measurements on self-ion ( $\text{Ga}^{++}$ ) implanted GaN epi-layers, with an emphasis on induced stress in the system. From our experimental results, we have estimated the hydrostatic strain coefficients inside the layers. In addition, we show the effect of disorder-activated Raman scattering in as-implanted samples and demonstrate the presence of a polar phonon-plasmon coupling in post-annealed implanted epi-layers.

## 2. Experimental Details

GaN epi-layers (pristine sample), of thickness 6  $\mu\text{m}$ , were grown on (0001)  $\text{Al}_2\text{O}_3$  substrate in a horizontal Metalorganic Chemical Vapor Deposition reactor at atmospheric pressure. Trimethylgallium (TMGa) was used as precursor with  $\text{NH}_3$  as reactant gas. The flow rate of  $\text{NH}_3$  was 3000 sccm. The low-temperature-deposited GaN buffer layer was first grown at 550C for about 30 min. Temperature was raised to 1050C and growth is continued for 8-10 hrs.

Ga<sup>++</sup> ions were implanted in these layers at 3.0 MeV with different fluences,  $1 \times 10^{15}$ ,  $2 \times 10^{15}$  and  $1 \times 10^{16}$  per cm<sup>2</sup> (Sample A - Sample C). The damage of the crystal lattice, induced by implantation, was removed by thermal annealing in flowing ultra-high pure N<sub>2</sub> at 650 °C for 15 minutes and subsequently at 1000 °C for 2 minutes [8]. The undoped and implanted epi-layers were found to be of n-type from Hall measurements with carrier concentration  $\sim 4\text{-}8 \times 10^{17}$  cm<sup>-3</sup>. Raman measurements were carried out at room temperature in a back-scattering geometry using a 488 nm air cooled Ar<sup>+</sup> laser as an excitation source. To avoid phase change in the samples by laser heating, the power density on the samples was tuned to  $3 \times 10^4$  Watt/m<sup>2</sup>. The Raman spectra were obtained using TRIAX550 single monochromator with an open electrode charge coupled device as a detector. With 150  $\mu$ m slit-width of the spectrometer, the accuracy of our Raman measurement is  $\pm 1.5$  cm<sup>-1</sup>.

### 3. Results and Discussion

#### 3.1. Pristine and self-ion implanted GaN epi-layer

Fig. 1 shows the Raman spectra of pristine and as-implanted GaN layers over a wavenumber range of 240 to 850 cm<sup>-1</sup>.

### Pristine GaN epi-layer:

Group theory predicts that for  $h$ -GaN there are eight phonon modes,  $2A_1 + 2B_1 + 2E_1 + 2E_2$ , at the  $\Gamma$  point. Except one  $A_1$  and one  $E_1$  mode (which are acoustic), the remaining six modes are optical. Optical  $A_1$  and  $E_1$  modes are both Raman and infrared active, while the two  $E_2$  modes are only Raman active and the two  $B_1$  modes are silent (Raman inactive). The higher frequency branch of the  $E_2$  phonon mode is denoted by  $E_2^H$  [9]. Peaks at 374, 416 and  $751\text{ cm}^{-1}$ , shown by \* marks in Fig. 1, are phonons from the sapphire substrate [10]. In the Raman spectrum of the pristine sample the line at  $568\text{ cm}^{-1}$  is due to the  $E_2^H$  mode. The Raman mode at  $345\text{ cm}^{-1}$  is not allowed by the  $C_{6v}$  space group in the first order Raman scattering at the zone center. This peak can be attributed to the 2nd order Raman scattering due to acoustic overtones in this region ( $300 - 420\text{ cm}^{-1}$ ) [11]. In the high frequency region for the pristine sample, we distinctly observe a feature at  $743\text{ cm}^{-1}$  (shown by double arrows in Fig. 1) due to the polar mode. This appears as a shoulder of the prominent peak at  $751\text{ cm}^{-1}$  from sapphire. The origin of this peak will be discussed latter.

### Self-ion implanted GaN epi-layers:

After ion-implantation the system loses its crystallinity and becomes disordered.

This is reflected in the broadening of the spectra of ion-implanted GaN layers

(Fig. 1). In addition, for as-implanted samples, we observe a broad band

at around  $290\text{ cm}^{-1}$ , which becomes prominent at higher fluences (inset of

Fig. 1). As a result of ion- irradiation, there is a slight rearrangement in the

lattice structure, hence, the wavevector conservation rule in Raman scattering

gets relaxed. The Raman spectrum reflects the total phonon density of states

(so called disorder-activated Raman scattering). The Raman-inactive modes

become Raman-active. Though silent for bulk  $\hbar$ -GaN, the phonon density of

states of the highest acoustic phonon branch at the zone boundary, the  $B_1^L$

mode, has a strong feature in the region  $290\text{-}300\text{ cm}^{-1}$  [12, 13, 14]. We assign

the above observed feature at around  $290\text{ cm}^{-1}$  to this  $B_1^L$  mode [1]. Due to

disorder-activated Raman scattering, the  $B_1^H$  mode also becomes allowed and

appears as a small hump around  $674\text{ cm}^{-1}$ , shown by  $\circ$  mark in Fig. 1 (See

phonon density of states in Ref. [14]). The polar mode at around  $740\text{ cm}^{-1}$  is

also broadened. In these as-implanted samples, the absence of Raman lines from

sapphire (substrate) indicates the effective “trapping” of the laser light inside the layers, which can affect the Raman scattering from the layers by changing the selection rules.

### 3.2. Post-annealed implanted samples

Raman spectra of the post-annealed GaN layers are shown in Fig. 2. After annealing, the disorder in samples gets reduced. All Raman modes in the low frequency region, discussed for the pristine sample, reappear distinctly in their spectra. In Raman spectra of post-annealed implanted samples the line at  $573\text{ cm}^{-1}$  is due to  $E_2^H$  mode, shifted by  $5\text{ cm}^{-1}$  from its value ( $568\text{ cm}^{-1}$ ) in bulk [9]. However, we do not observe any variation in spectral line-shape and position with implantation (Sample A - Sample C). Peaks from the sapphire substrate clearly reappear in these spectra. With the decrease in disorder in the annealed samples, the intensity of the peak at  $290\text{ cm}^{-1}$  due to the disorder-activated Raman scattering also decreases (inset of Fig. 2). However, we would like to point out that for *c*-GaN LA(X) and LA(L) (LA: longitudinal acoustic) modes appear at  $286\text{ cm}^{-1}$  and  $296\text{ cm}^{-1}$  [15]. The photoluminescence spectra of our samples (not shown here) do not carry a clear signature of the presence of cubic

phase in them.

### 3.3 LO phonon -plasmon coupling

In Fig. 3 we have shown Raman spectra in  $[z(y,y)\bar{z}]$  and  $[z(x,y)\bar{z}]$  configurations for Sample A. The low frequency acoustic mode at  $345\text{ cm}^{-1}$  and high frequency polar mode at  $743\text{ cm}^{-1}$  appear only in parallel polarization. Similar polarization dependence of the polar modes has been observed for all post-annealed implanted samples. In  $h$ -GaN, polar  $A_1(\text{LO})$  [LO:longitudinal optical] mode is expected to appear at  $733\text{ cm}^{-1}$  in  $[z(y,y)\bar{z}]$  configuration only. Assigning the observed feature at  $743\text{ cm}^{-1}$  to this  $A_1(\text{LO})$  mode is not justified, because the shift of a Raman line by  $10\text{ cm}^{-1}$  cannot be explained either by strain or zone folding effect [16]. Also, it is to be noted that this is the only peak for which the frequency shift is more than the shift for the other peaks in Fig. 2.

Undoped or nominally doped GaN is invariably of n-type, usually with a high free electron concentration ( $10^{17}$  -  $10^{18}\text{ cm}^{-3}$ ) at room temperature [17]. The coupling of collective electronic excitation (plasmon) and lattice vibration gives rise to the LO phonon-plasmon coupled mode. Such a mode in  $h$ -GaN shifts the LO phonon to the higher frequency [9]. Assigning the Raman line at



743 cm<sup>-1</sup> to the plasmon-A<sub>1</sub>(LO) phonon mode, we estimate the charge carrier density in Sample A using the empirical relation [9]

$$n = 1.1 \times 10^{17} (\Delta\omega)^{0.764}, \quad (1)$$

where,  $\Delta\omega$  is the observed frequency shift of the LO phonon. Taking  $\Delta\omega = 10$  cm<sup>-1</sup>, the  $n$  is estimated to be  $6 \times 10^{17}$  cm<sup>-3</sup>. which is also the value obtained from the Hall measurement. The above equation is valid for  $n \leq 1 \times 10^{19}$  cm<sup>-3</sup>.

Considering the contribution of the deformation potential within the lattice, a more precise evaluation of  $n$  can be carried out. The intensity of the Raman scattering is then given by [9, 18, 19]

$$I(\omega) = SA(\omega) \text{Im}[-1/\epsilon(\omega)], \quad (2)$$

where,  $\omega$  is the Raman shift and  $S$  is the proportionality constant. The dielectric function is

$$\epsilon(\omega) = \epsilon_\infty [1 + (\omega_L^2 - \omega_T^2)/(\omega_T^2 - \omega^2 - i\omega\Gamma) - \omega_P^2/(\omega^2 - i\omega\gamma)] = 0. \quad (3)$$

Here,  $\omega_T$  and  $\omega_L$  are the transverse optical (TO) and LO phonon frequencies for the uncoupled phonon modes.  $\epsilon_\infty$  is the high-frequency dielectric constant of GaN.  $\Gamma(\gamma)$  is the damping rate of the phonon (plasmon). The plasmon frequency

$\omega_P$  and  $A(\omega)$  are given by

$$\omega_p = [4\pi n e^2 / (\epsilon_\infty m^*)]^{1/2} \quad (4)$$

and

$$A(\omega) = 1 + 2C\omega_T^2[\omega_p^2\gamma(\omega_T^2 - \omega^2) - \omega^2\Gamma(\omega^2 + \gamma^2 - \omega_P^2)]/\Delta\omega \\ + C^2(\omega_T^4/\Delta\omega)[\omega_P^2[\gamma(\omega_L^2 - \omega_T^2) + \Gamma(\omega_P^2 - 2\omega^2)] + \omega^2\Gamma(\omega^2 + \gamma^2)]/(\omega_L^2 - \omega_T^2). \quad (5)$$

Here,  $C$  is the Faust-Henry coefficient, can be estimated from the ratio of the intensities of the polar LO and TO Raman scattering modes measured at  $90^\circ$  geometry [20]. The effective mass of the electron is  $m^* = 0.2m_0$ . All three parameters,  $\Gamma$ ,  $\gamma$  and  $n$ , are free parameters, which need to be chosen correctly, by fitting more than one Raman spectra of the layers with different carrier concentrations. Unfortunately, the Raman line shapes of all our post-annealed samples are nearly same, except, with higher implantation dose, a slight decrease in intensity of the coupled phonon-plasmon mode (modified  $A_1(LO)$  mode) is observed due to damping by the hole plasmon. In such a case, it was not possible to choose all three parameters,  $\Gamma$ ,  $\gamma$  and  $n$  meaningfully, to estimate more accurate value of  $n$  by following this procedure, compared to what we have obtained from Eqn. 1.

### 3.4 Stress Analysis

An epi-layer, of thickness  $6\text{ }\mu\text{m}$ , is not expected to exhibit a shift in the Raman line due to the effect of confinement of phonons [21]. Thus, the origin of the shift in Raman frequency from bulk samples can be either due to the presence of elastic strain or due to the change in interaction between the elastic medium and the macroscopic field. To eliminate the second factor we have investigated the non-polar  $E_2^H$  mode. It is important to note that within our experimental accuracy, all annealed  $\text{Ga}^{++}$  implanted GaN epi-layer exhibit nearly identical Raman spectra. Thus, the following stress analysis holds good for all post-annealed implanted samples.

GaN epi-layers grown on sapphire contain residual strains produced by mismatch in the lattice constants and thermal expansion coefficients between the GaN film and substrate [22]. Sufficient residual strain in the film induces formation of dislocations and stacking faults. Residual strain also leads to wafer bowing. It has been shown in Ref. [23] that for the above defects in a GaN layer of thickness  $1\text{ }\mu\text{m}$  (on sapphire substrate) the bi-axial strain energy varies from 0 (GaN surface) to 0.4 GPa (GaN/sapphire interface), indicating that the

surface layer is free from this type of strain. On the other hand, the ion irradiation induces strain in the film due to point defects. These defects are expected to be more near the surface of the layer. As the thickness of our films is 6  $\mu\text{m}$ , we attribute the shift in non-polar Raman mode only to the strain, generated by the point defects in the layer. These defects induce three dimensional stress, such as hydrostatic stress, if they are uniformly distributed. Based on the assumption of pure elastic theory (where Hooke's law is valid) the compressive stress can be calculated from the shift in  $E_2^H$  from [24]

$$\omega - \omega_0 = 4.17\sigma_H, \quad (6)$$

where,  $\sigma_H$  is the hydrostatic stress in GPa,  $\omega$  and  $\omega_0$  are the Raman line position of the stressed and unstressed samples. For a shift of 5  $\text{cm}^{-1}$  of the  $E_2^H$  mode between bulk GaN and ion-implanted layers we have estimated  $\sigma_H \approx 1.20$  GPa (see Table I).

Knowing  $\sigma_H$ , the hydrostatic strain tensor components,  $u_{xx}$  and  $u_{zz}$  (inplane and normal components of strain tensor) can be estimated from the following relations [25]

$$u_{xx} = u_{yy} = \sigma_H/Y \quad (7)$$

and

$$u_{zz} = -Ru_{xx}. \quad (8)$$

The Young's modulus,  $Y$ , of the material, in terms of elastic stiffness constants

$C_{ij}$  is given by [24]

$$Y = \frac{(C_{11} + C_{12})C_{33} - 2C_{13}^2}{C_{33} - C_{13}} \quad (9)$$

and  $R$  is the Poisson's ratio, can be written as

$$R = \frac{C_{11} + C_{12} - 2C_{13}}{C_{33} - C_{13}}. \quad (10)$$

Using Eqn. 7 to Eqn. 10, the strain tensor components have been estimated

and tabulated in Table I. Here, the elastic constants  $C_{ij}$  are taken to be  $C_{11} =$

396,  $C_{12} = 144$ ,  $C_{13} = 100$ , and  $C_{33} = 392$  GPa [26].

The change in frequency for a given phonon mode under symmetry conserv-

ing stress can be expressed in terms of strain tensor components and deformation

potentials constants ( $a_\lambda$  and  $b_\lambda$ ) as [24]

$$\omega - \omega_0 = 2a_\lambda u_{xx} + b_\lambda u_{zz}. \quad (11)$$

Furthermore, the bulk Grüneisen parameter  $\gamma_\lambda$  is related to the characteris-

tic phonon frequency at hydrostatic compression, phonon deformation potential

constants, and elastic constants of  $h$ -GaN by [7]

$$\gamma_\lambda = -\frac{2a_\lambda(C_{33} - C_{13}) + b_\lambda(C_{11} + C_{12} - 2C_{13})}{\omega_\lambda(C_{11} + C_{12} + 2C_{33} - 4C_{13})}. \quad (12)$$

For GaN,  $C_{33} + C_{13} = C_{11} + C_{12}$ . Therefore, from the above relation we get,

$$\gamma_\lambda = -\frac{2a_\lambda + b_\lambda}{3\omega_\lambda}. \quad (13)$$

The Grüneisen parameter used is  $\gamma_{E_2^H} = 1.54$  [7]. Knowing the values of strain tensor components, the deformation potential constants have been calculated to be  $-81 \text{ cm}^{-1}$  and  $-2486 \text{ cm}^{-1}$ .

With irradiation, we do not observe any noticeable change in the peak position and lineshape of non-polar Raman modes, which implies that no extra stress has been introduced in layers with increase in implantation fluence. The values of above parameters  $u_{xx}$ ,  $u_{zz}$ ,  $a_\lambda$  and  $b_\lambda$  are nearly same for all implanted samples.

### 3.5 Conclusion

We have performed first-order Raman measurements on  $\text{Ga}^{++}$  implanted GaN epi-layers. Raman lines become broadened after implantation. However, they reappear in all post-annealed implanted samples. We do not observe any change

in peak positions in Raman spectra of the films with an increase in implantation dose. Thus, the estimated hydrostatic stress and strain tensor components, obtained by us from the knowledge of phonon modes, are expected to hold good for all post-annealed implanted samples. It would have been interesting to check the stress analysis by high resolution x-ray diffraction measurements. We have also the disorder-activated Raman scattering in as-implanted samples. Interesting behavior of polar modes is reported for the post-annealed implanted samples.

### **Acknowledgements**

Authors thank Department of Science and Technology, India for financial assistance. SM also thanks Board of Research in Nuclear Science, India for financial support. SD thanks Y.C. Yu, Institute of Physics, Academia, Sinica, Taipei, Taiwan, for his help and also NSC, Taiwan, for financial assistance. Authors also thank the reviewers for their suggestions and comments.

\*E-mail:anushree@phy.iitkgp.ernet.in

<sup>†</sup>On leave from Materials Science Division, Indira Gandhi for Atomic Research,

Kalpakkam 603102, India. Email: [dhara@igcar.ernet.in](mailto:dhara@igcar.ernet.in).



# Bibliography

- [1] W. Limmer, W. Ritter, R. Saver, B. Mensching, C. Liu, and B. Rauschenbach, Appl. Phys. Lett. 72 (1998) 2589.
- [2] P. Perlin, T. Suski, H. Teisseyre, M. Leszczynski, I. Grzegory, J. Jun, S. Porowski, P. Boguslawski, J. Bernhole, J.C. Chervin, A. Polian, and T.D. Moustakas, Phys. Rev. Lett. 75 (1995) 296.
- [3] J. Neugebauer and C. van de Walle, Appl. Phys. Lett. 69 (1996) 503.
- [4] T. Mattila and R.M. Nieminen, Phys. Rev. B 55 (1997) 9571.
- [5] E.R. Glaser, T.A. Kennedy, K. Doverspike, L.B. Rowland, D.K. Gaskill, J.J.A. Freitas, M.A. Khan, D.T. Olson, J.N. Kuznia, and D.K. Wickenden, Phys. Rev. B 51 (1995) 13326.
- [6] Y.C. Chang, A.E. Oberhofer, J.F. Muth, M. Kolbas, and R.F. Davis, Appl. Phys. Lett. 79 (2001) 281.

- [7] V. Yu. Davydov, N.S. Averkiev, I.N. Goncharuk, D.K. nelson, I.P. Nikitina, A.S. Polkovnikov, A.N. Smirnov, M.A. Jacobson, and O.K. Semchinova, J. Appl. Phys. 82 (1997) 5097.
- [8] C. Liu, E. Alves, A.D. Sequeira, N. Franco, M.F. da Silva, and J.C. Soares, J. Appl. Phys. 90 (2001) 81.
- [9] H. Harima, J. Phys.: Condens. Matter 14 (2002) R967.
- [10] S.P.S. Porto and R.S. Krishnan, J. Chem. Phys. 47 (1967) 1009.
- [11] H. Siegle, G. Kaczmarczyk, L. Fillipidis, A.P. Litvinchuk, A. Hoffmann, and C. Thomsen, Phys. Rev. B 55 (1997) 7000.
- [12] C. Bungaro, K. Rapcewicz, and J. Bernhole, Phys. Rev. B 61 (2000) 6720.
- [13] H.M. Tütüncü and G.P. Srivastava, Phys. Rev. B 62 (2000) 5028.
- [14] K. Karch, F. Bechstedt, and T. Pletl, Phys. Rev. B 56 (1997) 3560.
- [15] J. Zi, X. Wan, G. Wei, K. Zhang, and X. Xie, J. Phys.: Condens. Matter 8 (1996) 6323.
- [16] H.D. Li, S.L. Zhang, H.B. Yang, G.T. Zou, Y.Y. Yang, K.T. Yue, X H. Wu, and Y. Yan, J. Appl. Phys. 91 (2002) 4562.

- [17] R. Poerschke (Ed.) Data in science and technology, Semiconductors Group  
IV elements and III-V compounds, Springer-Verlag Berlin Heidelberg, New  
York, 1991, p. 90.
- [18] M.V. Klein, B.N. Ganguly, and P.J. Colwell, Phys. Rev. B 6 (1972) 2380.
- [19] G. Irmer, V.V. Toporov, B.H. Bairamov, and J. Monecke, Phys. Status  
Solidi b 119 (1983) 595.
- [20] W.L. Faust and C.H. Henry, Phys. Rev. Lett. 17 (1966) 1265.
- [21] I.H. Campbell and P.M. Fauchet, Solid State Commun. 58 (1986) 739.
- [22] S. Strite and H. Morkoç, J. Vac. Sci. Technol. B 10 (1992) 1237.
- [23] H.J. Park, C. Park, S. Yeo, S.W. Kang, M. Mastro, O. Kryliouk, and T. J.  
Anderson, Phys. Stat. Sol. (c) 2 (2005) 2446.
- [24] J. Gleize, M. A. Renucci, J. Frandon, E. Bellet-Amalric, and B. Daubin, J.  
Appl. Phys. 93 (2003) 2065.
- [25] L.D. Landau and E.M. Lifshitz, (Translated by J.B. Sykes and W.H. Reid),  
Theory of Elasticity, Vol 7 of Course of Theoretical Physics, 3rd Ed. But-  
terworth Heinemann 1998.

[26] K. Kim, W.R.L. Lambrecht, and B. Segall, Phys. Rev. B 53 (1996) 16310.

### Figure Captions

Figure 1. Raman spectra of pristine (P) and as-implanted GaN epi-layers (Sample A - Sample C). The region between  $240\text{-}340\text{ cm}^{-1}$  is shown in the inset.

Figure 2. Raman spectra of pristine and post- annealed  $\text{Ga}^{++}$  implanted GaN epi-layers (Sample A- Sample C). The region between  $240\text{-}340\text{ cm}^{-1}$  is shown in the inset.

Figure 3. Polarization dependence of Raman modes in Sample A. Other implanted samples exhibit similar behavior.

**Table Caption**

Table I. Hydrostatic stress, phonon deformation potential constants and strain tensor components of postannealed  $\text{Ga}^{++}$  implanted GaN epi-layers.

Phonon Symmetry	$\omega - \omega_0$ ( $\text{cm}^{-1}$ )	$\sigma_H$ GPa	$a_\lambda$ $\text{cm}^{-1}$	$b_\lambda$ $\text{cm}^{-1}$	$u_{xx}$ $\times (10^{-3})$	$u_{zz}$ $\times (10^{-3})$
$E_2(\text{high})$	$5 \pm 1.5$	$1.20 \pm 0.36$	$-81 \pm 1$	$-2486 \pm 1$	$1.83 \pm 0.55$	$-2.13 \pm 0.64$

Table 1: Hydrostatic stress, phonon deformation potential constants and strain tensor components of  $\text{Ga}^{++}$  implanted GaN epi-layers.

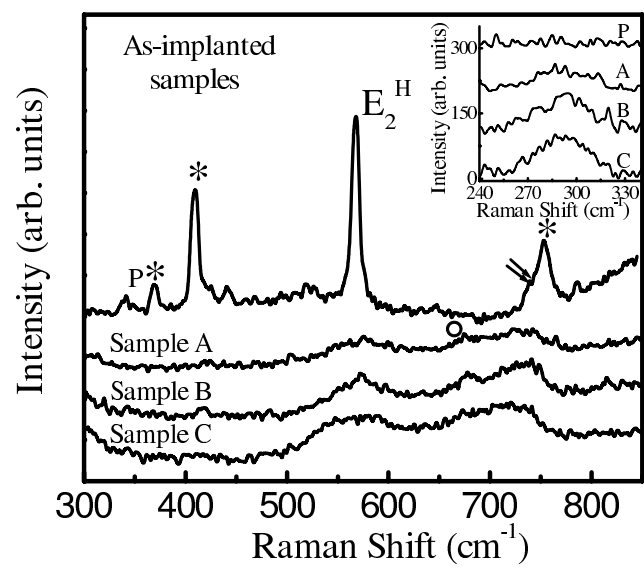


Figure 1. S. Mal *et al.*



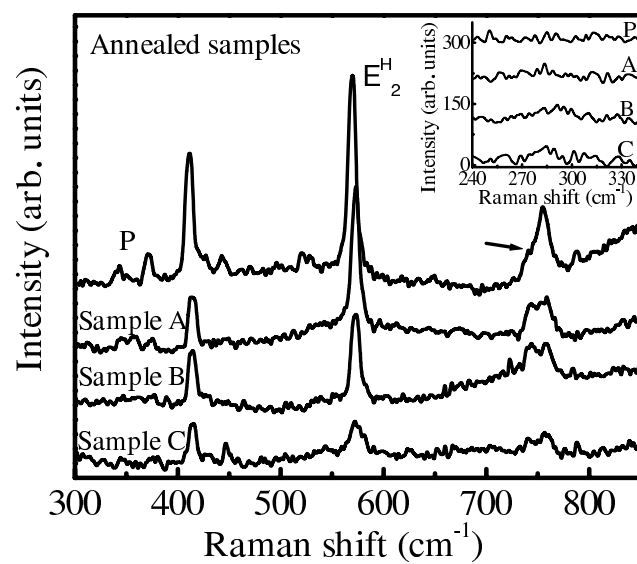


Figure 2. S. Mal *et al.*

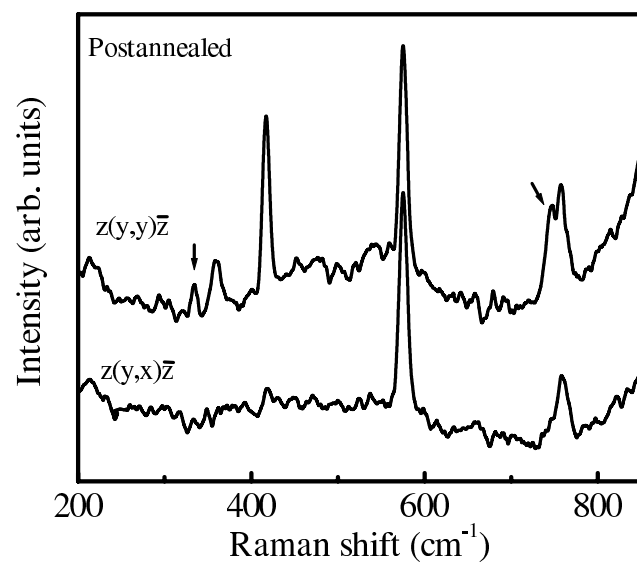


Figure 3. Mal *et al.*